Tailoring of the thermal expansion of $Cr_2(Al_x,Ge_{1-x})C$ phases

Thierry Cabioch, Per Eklund, Vincent Mauchamp, Michel Jaouen and Michel W. Barsoum

Original Publication:

Thierry Cabioch, Per Eklund, Vincent Mauchamp, Michel Jaouen and Michel W. Barsoum, Tailoring of the thermal expansion of $Cr_2(Al_x,Ge_{1-x})C$ phases, 2013, Journal of the European Ceramic Society, (33), 4, 897-904.
http://dx.doi.org/10.1016/j.jeurceramsoc.2012.10.008

Tailoring of the thermal expansion of $Cr_2(Al_x,Ge_{1-x})C$ phases

Thierry Cabioch[1,*], Per Eklund[2,†], Vincent Mauchamp[1], Michel Jaouen[1], and Michel W. Barsoum[1,3]

[1] *Institut Pprime, UPR 3346, Université de Poitiers, SP2MI-Boulevard 3, Téléport 2-BP 30179, 86962 Futuroscope Chasseneuil Cedex, France*
[2] *Thin Film Physics Division, Linköping University, IFM, 581 83 Linköping, Sweden*
[3] *Department of Materials Science and Engineering, Drexel University, Philadelphia, PA 19104, USA*

* Thierry.cabioch@univ-poitiers.fr
† Perek@ifm.liu.se

Abstract

We report thermal expansion coefficients of the end members and solid-solution compounds in the $Cr_2(Al_x,Ge_{1-x})C$ system. All samples studied were essentially phase-pure $Cr_2Al_xGe_{1-x}C$ except the Cr_2GeC sample, which contained a substantial fraction of $Cr_5Ge_3C_x$. X-ray diffraction performed in the 25 to 800 °C temperature range shows that the in-plane thermal expansion remains essentially constant at about $14\pm1\cdot10^{-6}$ K^{-1} irrespective of Al content. The thermal expansion of the *c* axis decreases monotonically from $17\pm1\cdot 10^{-6}$ K^{-1} for Cr_2GeC to $\sim12\pm1\cdot 10^{-6}$ K^{-1} with increasing Al content. At around the $Cr_2(Al_{0.75},Ge_{0.25})C$ composition, the thermal expansion coefficients along the two directions are equal; a useful property to minimize thermal residual stresses. This study thus demonstrates that a solid-solution approach is a route for tuning a physical property like the thermal expansion. For completeness, we also include a structure description of the $Cr_5Ge_3C_x$ phase, which has been reported before but is not well documented. Its space group is *$P6_3/mcm$* and its a and *c* lattice parameters are 7.14 Å and 4.88 Å, respectively. We also measured the thermal expansion coefficients of the $Cr_5Ge_3C_x$ phase. They are found to be $16.3\cdot10^{-6}$ K^{-1} and $28.4\cdot10^{-6}$ K^{-1} along the *a* and *c* axes, respectively. Thus, the thermal expansion coefficients of $Cr_5Ge_3C_x$ are highly anisotropic and considerably larger than those of the $Cr_2(Al_x,Ge_{1-x})C$ phases.

Keywords: Annealing, MAX phases, thermal expansion, Rietveld refinement, solid solution

I. Introduction

The family of phases known as $M_{n+1}AX_n$ phases (n = 1 – 3, or 'MAX phases') are a group of ternary early transition-metal (M) carbides and nitrides (X) interleaved with a group 12-16 element (A) [1,2,3,4]. The MAX phases have been extensively studied not only in order to shed light on their unique combination of properties but also to explore their potential for numerous industrial applications (see review articles [1,2,3,4] and recent examples [5,6,7,8,9,10,11,12,13]). It has long been appreciated that a promising strategy to tailor properties is to form solid solutions on the M, A and/or X sites [1,2]. However, practical examples of such property tuning are scarce, essentially limited to oxidation studies where the excellent oxidation resistance of the alumina-forming MAX phases Ti_2AlC and Ti_3AlC_2 is retained also for solid solutions, e. g., $Ti_3(Si,Al)C_2$ [14,15,16,17]. Solid-solution studies have mostly focused on exploring solid solution hardening effects [18,19,20,21,22,23], the evolution of the unit cell structure [24,25] or the possibility to synthesize new MAX phases [26,27,28,29]. Interestingly, with a few possible exceptions [30,31,32], solid solution hardening of the MAX phases does in general not appear to be pronounced. This issue is particularly evident in the Ti_3AC_2 systems with A = Si, Ge, Al, Sn, where numerous investigations [18,19,33,34,35] have demonstrated that solid solution hardening is not operative in these systems, while one study claims the opposite [32]. To advance the field, there is therefore a strong need for clear experimental evidence of solid-solution engineering to steer inherent materials properties.

The thermal expansion coefficients (TECs) of the MAX phases mainly fall in the range of ≈ 5 to $14 \cdot 10^{-6}$ K^{-1} [36]. The anisotropies of the TECs are relatively small for the Ti-containing MAX phases and become progressively higher as the average number of valence electrons increase (i.e., for M elements from groups 5 and 6 in the periodic table). In general, not much work has been carried out

on the effects of solid solutions on TECs. At $8.7 \cdot 10^{-6}\,K^{-1}$, the TECs of Ti_2AlC and Nb_2AlC are the same and marginally lower than that of their 50-50 solid solution at $8.9 \cdot 10^{-6}\,K^{-1}$ [37]. Similarly, it has been reported that substituting Ge for Si in Ti_3SiC_2 did not substantially affect the TECs of a 50-50 Si-Ge solid solution relative to the end members [33].

The main purpose of this work is to use a solid solution approach to tailor the thermal expansions of Cr_2GeC and Cr_2AlC. The rationale for choosing these two compounds is that both have relatively high and, especially Cr_2GeC, anisotropic TECs. Solids with high and anisotropic TECs tend to develop residual strains upon cooling. In some cases the residual strains can be so high as to result in the total failure of the solid [38]. The TEC of Cr_2GeC has been determined by measuring the temperature dependence of the lattice parameters obtained by x-ray diffraction (XRD) of powders [39] and from high temperature neutron diffraction [40], and is the highest of the known MAX phases. Both sets of experimental results are listed in Table. 1. However, the agreement between the two is not as good as most other MAX phases [39]. In passing, it is worth noting that the calculated thermal expansion coefficient [41] is more than 30 % larger than the highest experimental value.

The TEC of Cr_2GeC is the highest among all known MAX phases with an expansion along the *c* axis higher than in the basal plane. In contrast, in Cr_2AlC (also listed in Table 1), expansion along *a* is higher than along *c* [39]. It is therefore reasonable to assume that somewhere along the composition domain the two thermal expansions should cross. One could thus obtain a solid with isotropic thermal expansion and ideally eliminate the issues with residual strain upon cooling.

To this end, we have synthesized a series of $Cr_2Al_xGe_{1-x}C$ compounds (x = 0; 0.25; 0.5; 0.75; 1) and determined their structural parameters and thermal expansion coefficients from ambient temperature to 800 °C by *in-situ* XRD during annealing and Rietveld analysis of the data. Isotropic

thermal expansion is obtained around the composition of $Cr_2Al_{0.75}Ge_{0.25}C$. All samples studied were essentially phase-pure $Cr_2Al_xGe_{1-x}C$ except for the Cr_2GeC sample, which contained a substantial fraction of $Cr_5Ge_3C_x$. This phase is isostructural with $Ti_5Si_3C_x$ and has been known since the 1960s [42]. Although occasionally observed [43,44], its structure is not well documented in the literature. For completeness, we therefore also include its description as determined from Rietveld refinement.

II. Experimental Details

Five $Cr_2Al_xGe_{1-x}C$ compounds (x = 0; 0.25; 0.5; 0.75; 1) were synthesized using conventional powder metallurgy techniques. Powders of Cr, Al, Ge and C were weighed to obtain the nominal compositions: 2 Cr: 1.1xAl: 1.1(1-x) Ge and C. Al (325 mesh), Cr (particle size <10 μm) and Ge (100 mesh) powders are (Alfa Aesar) with a purities better than 99.5%, 99.8% and 99.999%, respectively. Erachem ensacco 250 granular powder (Chemwatch) was used as carbon powder. For all compositions, an excess of 10 wt.% Al and Ge was used to compensate for their loss by evaporation during the sintering process. The reactants were then mixed for 1 h in a shaker (Turbula™) and hand pressed (uniaxial cold compaction) to obtain cylinders, ~0.5 cm high and ~12 mm in diameter. The ~3-g cylinders had an open porosity close to 40 %. The five samples were placed together in a graphite furnace (Nabertherm™ GmbH, Lilienthal) and heated to 1400°C at 10°C/min and held at that temperature for 4 h.

The room temperature XRD patterns were obtained on a mechanically polished face of the samples in a Bragg-Brentano geometry using Cu Kα radiation. A Bruker D8 diffractometer operating at 40 kV and 40 mA was used. The 2θ range covered was 10 to 80°, with step intervals of 0.02° or 0.03° (2θ). Counting times between 5 s and 20 s for each angular step were used. To obtain the instrument

resolution function to account for the experimental broadening, an XRD pattern of a standard Cr_2O_3 powder (Standard NIST 600) was collected under the same geometrical conditions.

X-ray diffractograms in the 25 to 800 °C temperature range of the five samples were acquired under vacuum ($2x10^{-4}$ Pa) in a second diffractometer (X'PERT Philips) operating at 45 kV and 40 mA. An angular step size of 0.04°, with a count time of 4 s for each step, was used for the acquisition of diffractograms in the 35-50° 2θ range. The heights of the samples were adjusted prior to each X-ray measurement for consistent alignment. The setup is described in more detail elsewhere [45]. In short, the samples were placed on a resistively heated Ta filament with a calibrated Pt/Rh thermocouple clamped on the backside of the filament. A second Ta filament surrounding the sample was used to prevent temperature gradients.

Rietveld refinement of each diffractogram was performed using the Materials Analysis Using Diffraction (MAUD) software [46]. Such refinement resulted in precise determination of the unit-cell parameters at every temperature. The errors are estimated to be generally lower than $5 \cdot 10^{-4}$ Å or $2 \cdot 10^{-3}$ Å for the *a* and *c* lattice parameters, respectively. These uncertainties in turn were used to determine the uncertainties in the results presented herein. The *z* parameter of the Cr atoms, z_{Cr} (*z* or z_M in more general notation), in the unit cell was also deduced from Rietveld refinement of the diffractograms at room temperature. In this case, the error is estimated to be $< 5 \cdot 10^{-4}$, this last value being used as the uncertainty for the *z* values reported here.

The following equations were used to calculate the distortion parameters and the distance between the atoms (see Ref. [47]). Note that these equations are only valid for a M_2AX phase and are different for M_3AX_2 and M_4AX_3 phases. Distortion factor of the octahedron:

$$O_d = \frac{\sqrt{3}}{2\sqrt{4\, z_M^2 \left(\frac{c}{a}\right)^2 + \frac{1}{12}}} \qquad \text{(eq. 1)}$$

Distortion factor of the trigonal prisms:

$$P_d = \frac{1}{\sqrt{\frac{1}{3} + \left(\frac{1}{4} - z_M\right)^2 \left(\frac{c}{a}\right)^2}} \qquad \text{(eq. 2)}$$

Distance between M and A atoms:

$$d_{M-A} = \sqrt{\frac{a^2}{3} + c^2 \left(z_M - \frac{1}{4}\right)^2} \qquad \text{(eq. 3)}$$

Distance between M and X atoms:

$$d_{M-X} = \sqrt{\frac{a^2}{3} + c^2\, z_M^2} \qquad \text{(eq. 4)}$$

III. Results

The X-ray diffractograms of the samples tested are shown in Fig. 1. As previously mentioned, with the exception of Cr_2GeC (Fig. 1a), all other samples are predominantly single-phase. Rietveld analysis of the Cr_2GeC diffractograms showed the presence of about 41 wt. % $Cr_5Ge_3C_x$, a phase first reported by Jeitschko et al. [42]. Since the samples were porous and the lattice parameters were obtained from the Cr_2GeC peaks, the presence of this relatively large amount of secondary phase does not invalidate the results as evidenced by the good agreement in the TECs obtained here and those of Scabarozi et al. [39]. Why those of Lane et al. [40] are different is discussed below.

Figures 2a and b show the compositional dependence of the *a* and *c* lattice parameters, respectively. These results show that the *c* parameter increases with increasing Al content (Fig. 2a) while the *a* parameter decreases (Fig. 2b). Figure 2c shows the relative changes in *a*, *c*, *c/a* and unit cell volumes, V_{uc}, as a function of increasing Al content *x*. From these results it is clear that while c and c/a increase with *x*, V_{uc} remains essentially constant and the *a* lattice parameter decreases. The *z* parameter - the height position of Cr atoms in the unit cell - also monotonically increases with increasing Al-content (Fig. 2d).

Furthermore, making use of the values of *a*, *c* and *z* one can calculate the octahedral, O_d, and trigonal prisms, P_d, distortion parameters, as well as the distances between the Cr and Al or Cr and C atoms (equations (1-4)). Figures 2e and 2f show the results of these calculations. Strong distortions of the octahedral and trigonal prism sites are obtained for Cr_2GeC ($O_d \approx 1.12$; $P_d \approx 1.16$). The distortions, however, decrease with increasing Al content in the solid solution. As seen in Fig. 2f, the distance between the Cr and C atoms only weakly depends on the A element. On the contrary, a slight increase of the Cr-A distance is found when one progressively replaces Ge by Al.

In figures 3a and b, the temperature dependencies of the *a* and *c* lattice parameters, respectively, are plotted as a function of composition. These results were least-squares-fitted and converted to TECs along the *a* and *c* directions - α_a and α_c - respectively. The TECs are listed in Table 1 and plotted in Fig. 3c as a function of composition. From these results it is clear that the effect of increasing the Al-content on α_c is higher than on α_a, the latter remaining almost constant. Significantly, the two values are equal around the $Cr_2(Al_{0.75}Ge_{0.25})C$ composition.

As noted above, our Cr_2GeC samples contained a large (~40 wt. %) phase fraction of $Cr_5Ge_3C_x$ phase. Jeitschko et al. [42] reported this phase and found it to be isostructural to $Ti_5Si_3C_x$ with space group *P6₃/mcm* but without presenting the complete structure description. Here, we confirm this structure. For completeness, the structural parameters of $Cr_5Ge_3C_x$ determined from the Rietveld refinement are listed in Table 2. The occupancy of all sites is assumed to be 1. This may not be valid for the C sites, but virtually no difference in the refinement is obtained by allowing the C occupancy to vary because of the low scattering factor of the light C atoms that thus have a limited contribution to the diffraction. Thus, a conclusive determination of the C occupancy is not possible. At room temperature, the *a* and *c* lattice parameters were found to be 7.14 Å and 4.88 Å, respectively. Figure 4 shows the evolution of the *a* and *c* lattice parameters with temperature. The thermal expansion coefficients of the $Cr_5Ge_3C_x$ phase, listed in Table 1, are high and quite anisotropic. For comparison, the isostructural $Ti_5Si_3C_x$ phase has thermal expansion coefficients $\alpha_a = 9.4 \cdot 10^{-6}$ K^{-1} and $\alpha_c = 17.8 \cdot 10^{-6}$ K^{-1} [48].

IV. Discussion

The most important result of this work is the possibility of compositionally fine-tuning the TECs α_a and α_c so as to render them virtually equal (i.e., isotropic). For all intents and purposes, it is reasonable to assume that the $Cr_2(Al_{0.75},Ge_{0.25})C$ composition would respond to temperature variations as if it were a cubic solid. The most important benefit of this feature is the absence of residual stresses at room temperature when cooling from higher temperatures.

In a recent paper on the thermal properties of Cr_2GeC [40] it was conceded that the reason the TECs obtained from XRD were larger than those obtained from neutron diffraction was unclear. One possibility, always present, is sample-to-sample variations. Other possibilities are secondary phases and effects of non-stoichiometry, the latter known to occur for several other MAX phases [25, 49]. However, our present TEC results are similar to those of Scabarozi et al. [39]. It is therefore unlikely that the discrepancies are due to sample-to-sample variations. The variations must thus be traced to the method of investigation. In contradistinction to the neutron-diffraction work [40] where a *bulk* dense sample was used, here a highly porous sample was used instead. Given the high anisotropies of the TECs it is reasonable to assume that upon cooling of the bulk sample micro-strains developed that reduced both α_a and α_c as observed (Table 1). This conclusion also partially explains why the agreement between the TEC values obtained from dilatometry and those measured using XRD is reasonable for most of the MAX phases, but not for Cr_2GeC and Nb_2AsC [39]. With an α_a of 2.9×10^{-6} K^{-1} and an α_c of 10.6×10^{-6} K^{-1}, Nb_2AsC has a very high degree of anisotropy in thermal expansion. Said otherwise, the larger the TECs, the larger the difference one would expect between the TECs measured on a powder and those measured on bulk samples, whether by diffraction techniques or dilatometry.

It is generally considered that the MAX phases can form isostructural solid solution on all sites. It is then assumed that a random solid solution is obtained irrespective of site although it has been proposed that some ordering could occur on the X sites in $Ti_2Al(C_xN_{1-x})$ but with a small ordering energy so that it is generally not observed experimentally [50]. It is therefore likely the same for our case and our XRD results can be simply explained assuming a random solid solution on the A site. Furthermore, it was not necessary to introduce microstrains to fit the data during Rietveld refinement of the diffractograms, a result which is consistent with the absence of compositional or strain gradients in our samples.

The linear evolution of *a*, *c* and *c/a*, with increasing Al content (Fig. 2c) is not a general trend in MAX phases even if it is also the case for $(Ti_{1-x},V_x)_2AlC$ and $(V_{1-x},Cr_x)_2AlC$ solid solutions [24]. For instance, the *a* lattice parameter varies linearly as a function of *x* in $Ti_2Al(C_xN_{1-x})$ [25] but not the *c* lattice parameter. Neither *a* nor *c* vary linearly with *x* for $(Ti_{1-x},Cr_x)_2AlC$ compounds [24]. Therefore, there are no general simple rules or empiric laws that predict the evolution of the lattice parameters. What should obey Vegard's law in MAX-phase solid solutions is the interatomic distance between the elements, as is the case here. There is no other systematic study of the evolution of the *z* parameter in MAX-phase solid solutions, so general conclusions cannot be drawn on this point. In the present case, knowledge of the evolution of the *z* parameter is of interest since it allows following the evolution of the interatomic distance between the different atomic species. Based on this analysis and the results in Fig. 2f, the following conclusions can be reached: the Cr-C interatomic distance does not depend on *x* in the $Cr_2(Al_x,Ge_{1-x})C$ compounds whereas the distance between Cr and A atoms progressively increases with *x*. This is expected since the M-A bonds are generally weaker than the M-X ones; the strong M-X bond is not very sensitive to A modifications in solid solutions.

In general, TECs are intimately related to the interatomic bond strengths. In the frame of previous considerations, one should immediately propose that the thermal expansion of the Cr-C interatomic bonds should be lower than those of the Cr-A ones. Nevertheless, the knowledge of the TECs for the interatomic bondings ($\alpha_{Cr\text{-}C}$ and $\alpha_{Cr\text{-}A}$ where A = Al or Ge in the present case) cannot be simply deduced from α_a and α_c since they depend on the z parameter, which changes with temperature, as in the following general expressions:

$$\alpha_{M-A}=\frac{1}{d_{M-A}^2}\left(\frac{a^2}{3}\alpha_a+c^2\left(z_M-\frac{1}{4}\right)^2\left(\alpha_c+\frac{z_M}{z_M-\frac{1}{4}}\alpha_{Z_M}\right)\right), \quad \text{(eq. 5)}$$

$$\alpha_{M-X}=\frac{1}{d_{M-X}^2}\left(\frac{a^2}{3}\alpha_a+c^2 z_M^2\left(\alpha_c+\alpha_{Z_M}\right)\right), \quad \text{(eq. 6)}$$

where

$$\alpha_{Z_M}=\frac{1}{z_M}\frac{\partial z_M}{\partial T}, \quad \text{(eq. 7)}$$

and M, A and X represent atomic species from a $M_{n+1}AX_n$ phase with n = 1.

In this work, α_a and α_c are known, whereas α_{zM} would ideally be deduced from the refinement of the z parameter as a function of the temperature T. However, the small 2θ range chosen, as well as the quite high acquisition rates required at high temperatures to minimize the effects of thermal drift did not allow for the precise determination of z_M as a function of T. However, the fact that the intensity

ratios of the different diffraction peaks did *not* vary with increasing *T* is taken as evidence that the relative position of the Cr atoms in the unit cell, i.e. z, remains essentially constant or varies only slightly with increasing temperature. This is supported by preliminary neutron-diffraction results on Cr_2GeC indicating that the value of α_{Z_M} is close to $-6 \cdot 10^{-6}$ K^{-1} [51]. This value leads to a change of $4x10^{-4}$ for z_{Cr} between room temperature ($z_{Cr} = 0.0844$) to 800°C ($z_{Cr} = 0.084$). Such small variations are below the resolution of our experiment. Note that even such a small change in *z* induces strong modifications for the $\alpha_{Cr\text{-}C}$ and $\alpha_{Cr\text{-}A}$ values. In other words, it is not possible to unambiguously discuss the evolution of $\alpha_{Cr\text{-}C}$ and $\alpha_{Cr\text{-}A}$ as a function of the Al content without a precise determination of $\alpha_{Z_{Cr}}$ for every composition. Similarly, it is not possible to calculate the evolution of the distortion parameters O_d and P_d with temperature. Nevertheless, by considering values of 10^{-5} K^{-1} for $\alpha_{Z_{Cr}}$, it is possible to conclude that these distortion parameters remain very close to the values obtained at room temperature.

Despite these limitations (i.e. we cannot fully discuss the evolution of the Cr-A and Cr-C interatomic distance with the temperature), room temperature observations show that Cr-C bonds are weakly influenced by the Cr-Al or Cr-Ge bonds. It is then reasonable to propose that the Cr-Al bonds are stronger than the Cr-Ge bonds. This important conclusion is consistent with the following facts:

a) The thermal expansion along [001] in Cr_2AlC is lower than in Cr_2GeC (Fig. 3c)
b) At ≈ 285 GPa, the Young's modulus of Cr_2AlC [52,53,54] is significantly higher than that of Cr_2GeC at 245 GPa [55].
c) The shear modulus of Cr_2AlC is reported to be 102 GPa [56], 116 GPa [53], and 121 GPa [57]. Even though there is some spread in these experimental data, it is clear that the shear modulus of Cr_2AlC is significantly higher than that of Cr_2GeC at ≈ 80 GPa [55].

This conclusion is apparently at odds with bulk moduli, B, results. At 166 GPa, the bulk modulus of Cr_2AlC [56], is equal to or lower than that reported for Cr_2GeC (169 GPa [58] to 182 GPa [59]).The reason for this observation is unclear, but might be related to the presence a significant concentration of point defects on one of the Cr_2AlC sublattices. An indirect support of this conclusion is that the Young's modulus measured for Cr_2AlC in Ref. [56] is significantly lower than other reports [53,57] on the same material.

It should also be stressed that care must be taken when comparing experimental results on bulk and shear moduli with theoretical calculations of these parameters. Most theoretical studies on MAX phases [60,61,62,63] do not account for magnetism or strong electron-correlation effects, assumptions that are valid for MAX phases with M elements from group 4 or 5 (e.g., Ti, Nb, V). Neglecting these effects, however, strongly affect the results for the Cr-based MAX phases [41,64,65].

Lastly, we are faced with the following paradox. At 2.656 Å, the Cr-Al bond is longer than the C-Ge bond at 2.632 Å. Typically, bond distances cannot be directly related to bond strengths, lengths, etc. because the atomic radii of the elements generally differ. It is thus crucial, and fundamental, to the foregoing discussion to note that at 1.25 Å, the radii of the Al and Ge atoms are *identical*. It follows that, based on bond-length criteria alone, one would expect the Cr-Al bond to expand faster with increasing temperature, when in fact it does not (Fig. 3c). This implies that other factors, such as the distortion of the octahedra or trigonal prisms, come into play. Clearly more work is needed, both theoretical and experimental, to resolve this interesting paradox.

V. Summary and Conclusions

Using XRD and Rietveld analysis we have determined the lattice parameters as a function of x and temperature for $Cr_2(Al_x,Ge_{1-x})C$ compounds including the two end members. At room temperature, the *a* and *c* lattice parameters and the *c/a* ratio vary linearly with x. Whereas the Cr-A interatomic distance increases with x (A = Al and/or Ge), the length of the Cr-C interatomic bonding remains constant. With increasing Al-content, the thermal expansion along the *a* direction is essentially constant at about $14\pm1 \cdot 10^{-6}$ K^{-1}. The *c* lattice-parameter thermal expansion, on the other hand, decreases monotonically from $17\pm1 \cdot 10^{-6}$ K^{-1} to about $12\pm1 \cdot 10^{-6}$ K^{-1} with increasing Al content.

The most important result of this work is the demonstration of compositional tuning of the thermal expansion coefficients so as to render them virtually isotropic for the $Cr_2(Al_{0.75},Ge_{0.25})C$ composition. This compound should thus respond to temperature variations like a cubic solid, which has the key benefit of absence of residual stresses at room temperature when cooling from higher temperatures.

Acknowledgments

The Swedish Research Council (VR) Linnaeus LiLi-NFM Strong Research Environment is acknowledged for base funding (P.E.) and for a visiting researcher position for T.C. M.W.B. would like to thank the University of Poitiers for a Visiting Professor position.

References

[1] Barsoum MW. The $M_{N+1}AX_N$ Phases: A New Class of Solids; Thermodynamically Stable Nanolaminates. *Prog Solid State Chem* 2000**;28;**201-80
[2] Eklund P, Beckers M, Jansson U, Högberg H, Hultman L. The Mn+1AXn phases: materials science and thin film processing. *Thin Solid Films* 2010**;518:**1851-78
[3] Barsoum MW, M. Radovic M. Elastic and Mechanical Properties of the MAX Phases, *Annu Rev Mater Res* 2011**;41:**195-227.
[4] Sun ZM, Progress in research and development on MAX phases—a family of metallic ceramics. *Int Mater Rev* 2011;**56:**143-66
[5] Drevin-Bazet A, Barbot JF, Alkazaz M, Cabioc'h T, Beaufort MF. Epitaxial growth of Ti_3SiC_2 thin films with basal planes parallel or orthogonal to the surface on α -SiC. *Appl Phys Lett* 2012**;101:**021606.
[6] Buchholt K, Ghandi R, Domeij M, Zetterling C-M, Lu J, Eklund P, Hultman L, Lloyd Spetz A. Ohmic contact properties of magnetron sputtered Ti_3SiC_2 on n- and p-type 4H-silicon carbide. *Appl Phys Lett* 2011;**98:**042108.
[7] Grieseler RM, Kups T, Wilke M, Hopfeld M, Schaaf P. Formation of Ti_2AlN nanolaminate films by multilayer-deposition and subsequent rapid thermal annealing. *Mater Lett* 2012;**82**:74-77
[8] Yang HJ, Pei YT, Song GM, De Hosson JM. Healing performance of Ti_2AlC ceramic studied with in situ mcirocantilever bending *J Eur Ceram Soc* 2012, DOI:10.1016/j.jeurceramsoc.2012.09.012
[9] Yang HJ, Pei YT, Song GM, De Hosson JM. Self-healing performance of Ti_2AlC ceramic *J Mater Chem* 2012;**22**:8304-13
[10] Eklund P, Dahlqvist M, Tengstrand O, Hultman L, Lu J, Nedfors N, Jansson U, Rosén J. Discovery of the ternary nanolaminated compound Nb_2GeC by a systematic theoretical-experimental approach. *Phys Rev Lett* 2012;**109:**035502
[11] Magnuson M, Mattesini M, van Nong N, Eklund P, Hultman L. The electronic-structure origin of the anisotropic thermopower of nanolaminated Ti_3SiC_2 determined by polarized x-ray spectroscopy and Seebeck measurements. *Phys Rev B* 2012;**85:**195134.
[12] To Baben M, Shang L, Emmerlich J, Schneider JM. Oxygen incorporation in M_2AlC (M = Ti, V, Cr). *Acta Mater* 2012;**60:**4810-18
[13] Mauchamp V, Bugnet M, Chartier P, Cabioc'h T, Jaouen M, Vinson J, Jorssien K, Rehr JJ. Interplay between many-body effects and charge transfers in Cr_2AlC bulk plasmon exciton. *Phys Rev B* 2012;**86**:125109.
[14] Lee DB, Nguyen TD, Park SW. High-temperature oxidation of Ti3Al0.5Si0.5C2 compounds between 900 and 1200 °C in air. *J Alloys Compds* 2009;**469**:374-9.
[15] Zheng LL, Sun LC, LI MS, Zhou YC. Improving the High-Temperature Oxidation Resistance of $Ti_3(SiAl)C_2$ by Nb-Doping. *J Amer Ceram Soc* 2011**;94:**3579-86.
[16] Zhang HB, Zhou YC, Bao YW, Li MS. Improving the oxidation resistance of Ti_3SiC_2 by forming a $Ti_3Si_{0.9}Al_{0.1}C_2$ solid solution. *Acta Mater* 2004**;52:**3631-7.
[17] Li SB, Song GM, Zhou Y. A dense and fine-grained $SiC/Ti_3Si(Al)C_2$ composite and its high-temperature oxidation behavior. *J Eur Ceram Soc* 2012**;32:**3435-44.
[18] Bei GP, Gauthier-Brunet V, Tromas C, Dubois, S. Synthesis, Characterization, and Intrinsic Hardness of Layered Nanolaminate Ti_3AlC_2 and $Ti_3Al_{0.8}Sn_{0.2}C_2$ Solid Solution. *J Amer Ceram Soc* 2012**;95:**102-7.
[19] Ganguly A, Zhen T, Barsoum MW. Synthesis and mechanical properties of Ti_3GeC_2 and $Ti_3(Si_xGe_{1-x})C_2$ (x = 0.5, 0.75) solid solutions *J Alloys Compds* 2004;**376:**287-95.
[20] Manoun B, Leaffer O, Gupta S, Hoffman E, Saxena SK, Spanier J, Barsoum MW. On the compression behavior of Ti2InC, (Ti0.5, Zr0.5)2InC, and M2SnC (, Nb, Hf) to quasi-hydrostatic pressures up to 50 GPa. *Solid State Comm* 2009;**149:**1978-81
[21] Radovic M, Ganguly A, Barsoum MW. Elastic properties and phonon conductivities of $Ti_3Al(C_{0.5},N_{0.5})_2$ and $Ti_2Al(C_{0.5},N_{0.5})$ solid solutions *J Mater Res* 2008;**23:**1517-21.

[22] Salama I, El-Raghy T, Barsoum MW. Synthesis and mechanical properties of Nb_2AlC and $(Ti,Nb)_2AlC$ *J Alloys Compds* 2002;**347:**271-8.
[23] Zhou AG, Barsoum MW. Kinking nonlinear elastic deformation of Ti_3AlC_2, Ti_2AlC, $Ti_3Al(C_{0.5},N_{0.5})_2$ and $Ti_2Al(C_{0.5},N_{0.5})$. *J Alloys Compds* 2010;**498:**62-70.
[24] Schuster JC, Nowotny H, Vaccaro C. The ternary systems: CrAlC, VAlC, and TiAlC and the behavior of H-phases (M_2AlC) *J Solid State Chem* 1980;**32:**213-9.
[25] Cabioc'h T, Eklund P, Mauchamp V, Jaouen M. Structural investigation of substoichiometry and solid solution effects in $Ti_2Al(C_x,N_{1-x})_y$ compounds. *J Eur Ceram Soc* 2012;**32:**1803-11.
[26] Zhou Y, Meng F, Zhang J. New MAX-Phase Compounds in the V–Cr–Al–C System. *J Amer Ceram Soc* 2008;**91:**1357-60.
[27] Zheng L, Wang J, Lu X, Li F, Wang J, Zhou Y. $(Ti_{0.5}Nb_{0.5})_5AlC_4$: A New-Layered Compound Belonging to MAX Phases *J Amer Ceram Soc* 2010;**93:**3068-71.
[28] Phatak NA, Saxena SK, Fei Y, Hu J. Synthesis of a new MAX compound $(Cr_{0.5}V_{0.5})_2GeC$ and its compressive behavior up to 49 GPa. *J Alloys Compds* 2009;**475:**629.
[29] Kerdsongpanya S, Buchholt K, Tengstrand O, Lu J, Jensen J, Hultman L, Eklund P. Phase-stabilization and substrate effects on nucleation and growth of $(Ti,V)_{n+1}GeC_n$ thin films. *J Appl Phys* 2011;**110:**053516
[30] Barsoum MW, Ali M, El-Raghy T. Processing and characterization of Ti_2AlC, Ti_2AlN, and $Ti_2AlC_{0.5}N_{0.5}$ *Met Mater Trans* 2000;**31A:**1857-65.
[31] Meng FL, Zhou YC, Wang JY. Strengthening of Ti2AlC by substituting Ti with V. *Scripta Mater* 2005;**53:**1369-72.
[32] Zhou YC, Chen JX, Wang JY. Strengthening of Ti_3AlC_2 by incorporation of Si to form $Ti_3Al_{1-x}Si_xC_2$ solid solutions. *Acta Mater* 2006;**54:**1317-22.
[33] Finkel P, Seaman B, Harrell K, Palma J, Hettinger JD, Lofland SE, Ganguly A, Barsoum MW, Sun Z, Li S, Ahuja R. Electronic, thermal, and elastic properties of $Ti_3Si_{1-x}Ge_xC_2$ solid solutions. *Phys Rev B* 2004;**70:**085104.
[34] Dubois S, Pei GP, Tromas C, Gauthier-Brunet V, Gadaud P. Synthesis, Microstructure, and Mechanical Properties of $Ti_3Sn_{1-x}Al_xC_2$ MAX Phase Solid Solutions. *Int J Appl Ceram Technol* 2010;**7:**719-29.
[35] Radovic M, Barsoum MW, Ganguly A, Zhen T, Finkel P, Kalindini SR, Lara-Curzio E. On the elastic properties and mechanical damping of Ti_3SiC_2, Ti_3GeC_2, $Ti_3Si_{0.5}Al_{0.5}C_2$ and Ti_2AlC in the 300–1573 K temperature range. *Acta Mater* 2006;**54**:2757-67.
[36] Barsoum MW, The MAX Phases and Their Properties, in: Chen I-W (Ed.), Ceramics Science and Technology, Vol. 2: Properties, Wiley-VCH Verlag GmbH & Co, 2010.
[37] Barsoum MW, Salama I, El-Raghy T, Golczewski J, Porter WD, Wang H, Siefert H, Aldinger F. Thermal and electrical properties of Nb_2AlC, $(Ti, Nb)_2AlC$ and Ti_2AlC *Met Mater Trans* 2002;**33a:**2775-9.
[38] Barsoum MW (2003). Fundamentals of Ceramics (Bristol, Institute of Physics).
[39] Scabarozi TH, Amini S, Leaffer O, Ganguly A, Gupta S, Tambussi W, Clipper S, Spanier JE, Barsoum MW, Hettinger JD, Lofland SE. Thermal expansion of select $M_{n+1}AX_n$ (M = early transition metal, A = A group element, X = C or N) phases measured by high temperature x-ray diffraction and dilatometry. *J Appl Phys* 2009;**105:**013543.
[40] Lane NJ, Vogel SC, Barsoum MW. Temperature-Dependent Crystal Structures of Ti_2AlN and Cr_2GeC as Determined from High Temperature Neutron Diffraction. *J Amer Ceram Soc* 2011;**94:**3473-9.
[41] Zhou W, Liu LJ, Wu P. First-principles study of structural, thermodynamic, elastic, and magnetic properties of Cr_2GeC under pressure and temperature *J Appl Phys* 2009;**106:**033501.
[42] Jeitschko W, Nowotny H, Benesovsky F. Kohlenstoffhaltige ternäre Verbindungen (V-Ge-C, Nb-Ga-C, Ta-Ga-C, Ta-Ge-C, Cr-Ga-C und Cr-Ge-C). *Monatsh Chem* 1963;**94:**844.
[43] T. H. Scabarozi, "Combinatorial Investigation of Nanolaminate Ternary Carbide Thin Films" PhD thesis, Drexel University, Philadelphia, PA, USA, 2009. Available online through http://idea.library.drexel.edu/
[44] Eklund P, Bugnet M, Mauchamp V, Dubois S, Tromas C, Jensen J, Piraux L, Gence L, Jaouen M, Cabioc'h T. Epitaxial growth and electrical transport properties of Cr_2GeC thin films. *Phys Rev B* 2011;**84:**075424.
[45] Emmerlich J, Music D, Eklund P, Wilhelmsson O, Jansson U, Schneider JM, Högberg H, Hultman L. Thermal stability of Ti_3SiC_2 thin films. *Acta Mater* 2007;**55:**1479-88
[46] Lutterotti L, Matthies L, Wenk HR, Schultz AS, Richardson JW. Combined texture and structure analysis of deformed limestone from time-of-flight neutron diffraction spectra. *J Appl Phys* 1997;**81:**594-600.
[47] Kanoun MB, Goumri-Said SB, Jaouen M. Steric effect on the M site of nanolaminate compounds M_2SnC (M = Ti, Zr, Hf and Nb) *J Phys: Condens Matter* 2009;**21:**045404.
[48] Thorn AJ, Akinc M, Cavin OB, Hubbard CR. Thermal expansion anisotropy of Ti_5Si_3. *J Mater Sci Lett* 1994;**13:**1657-60.
[49] Buchholt K, Eklund P, Jensen J, Lu J, Ghandi R, Domeij M, Zetterling CM, Behan G, Zhang H, Lloyd Spetz A, Hultman L. Growth and characterization of epitaxial Ti_3GeC_2 thin films on 4H-SiC(0001). *J Cryst Growth* 2012;**343:**133-7.
[50] Arróyave R, Radovic M. 5.Ab initio investigation of $Ti_2Al(C,N)$ solid solutions. *Phys Rev B* 2011;**84:**134112.
[51] Lane NJ, private communication.

[52] Lin ZJ, Zhou YC, Li MS. Synthesis, Microstructure, and Property of Cr_2AlC. *J Mater Sci Tech* 2007;**23:**721-46.
[53] Tian W, Wang P, Zhang G, Kan Y, Li Y. Mechanical Properties of Cr_2AlC Ceramics. *J Amer Ceram Soc* 2007**;90:**1663-6.
[54] Ying G, He X, Li M, Du S, Han W, He F. Effect of Cr_7C_3 on the mechanical, thermal, and electrical properties of Cr_2AlC. *J Alloys Compds* 2011;**509**:8022-7.
[55] Amini S, Zhou A, Gupta S, DeVillier A, Finkel P, Barsoum MW. Synthesis and elastic and mechanical properties of Cr_2GeC *J Mater Res* 2008;**23**:2157-65.
[56] Manoun B, Gulve RP, Saxena SK, Gupta S, Barsoum MW, Zha CS. Compression behavior of M2AlC (M=Ti, V, Cr, Nb, and Ta) phases to above 50 GPa. *Phys Rev B* 2006;**73:**024110
[57] Lin ZJ, Li MS, Wang JY, Zhou YC. High-temperature oxidation and hot corrosion of Cr_2AlC. *Acta Mater* 2007;**55**:6182-91.
[58] Phatak NA, Kulkarni SR, Drozd V, Saxena SK, Deng L, Fei Y, Hu J, Luo W, Ahuja R. Synthesis and compressive behavior of Cr_2GeC up to 48 GPa. *J Alloys Compds* 2008;**463:**220-5.
[59] Manoun B, Amini S, Gupta S, Saxena SK, Barsoum MW. On the compression behavior of Cr_2GeC and V_2GeC up to quasi-hydrostatic pressures of 50 GPa. *J Phys: Conden Matter*, 2007;**19:**456218.
[60] Bouhemadou A. Calculated structural, electronic and elastic properties of M2GeC (M=Ti, V, Cr, Zr, Nb, Mo, Hf, Ta and W) *Appl Phys A* 2009;**96:**959-67.
[61] Cover MF, Warschkow O, Bilek MMM, McKenzie DR. A comprehensive survey of M_2AX phase elastic properties. *J Phys: Cond. Matter* 2009;**21:**305403.
[62] Jia GZ, Yang LJ. Ab initio calculations for properties of Ti_2AlN and Cr_2AlC. *Physica B* 2010;**405:**4561-4.
[63] Sun Z, Li S, Ahuja R, Schneider JM. Calculated elastic properties of M_2AlC (M=Ti, V, Cr, Nb and Ta). *Solid State Comm* 2004;**129:**589-92.
[64] Du YL, Sun ZM, Hashimoto H, Barsoum MW. Electron correlation effects in the MAX phase Cr_2AlC from first-principles. *J Appl Phys* 2011;**109:**063707.
[65] Ramzan M, Lebègue S, Ahuja R. Correlation effects in the electronic and structural properties of Cr_2AlC. *Phys Stat Sol RRL* 2011;**5;**122-4

Table 1: Summary of room temperature lattice parameters and thermal expansion coefficients of compounds explored in this work. Also included are previously reported values.

Compound	a (Å)	c (Å)	α_a $(K)^{-1}$ $x10^{-6}$	α_c $(K)^{-1}$ $x10^{-6}$	$(2\alpha_a+\alpha_c)/3$ $x10^{-6}$	Ref.
Cr_2GeC	2.9529	12.110	14.3 12.9 12.3	17.2 17.6 14.4	15.27 14.47 13.00	This work Scabarozi et al. [39] Lane et al. [40]
$Cr_2(Al_{0.25}Ge_{0.75})C$	2.9396	12.212	14.8	15.7	15.00	This work
$Cr_2(Al_{0.5}Ge_{0.5})C$	2.9091	12.437	13.4	14.8	13.87	This work
$Cr_2(Al_{0.75}Ge_{0.25})C$	2.8796	12.646	13.4	13.0	13.27	This work
Cr_2AlC	2.862	12.817	13.3 12.8	11.7 12.1	12.77 12.57	This work Scabarozi et al. [39]
$Cr_5Ge_3C_x$	7.14 7.6	4.88 4.86	16.3	28.4	20.3	This work Scabarozi, thesis [43]

Table 2: Structural parameters of $Cr_5Ge_cC_x$.

Atom	Site	x	y	z	Occupancy
Cr(1)	4d	1/3	2/3	0	1
Cr(2)	6g	0.237	0	1/4	1
Ge	6g	0.6	0	1/4	1
C	2b	0	0	0	1
Space group : $P6_3/mcm$ (n°193) a= 7.14 Å c= 4.88 Å					

Figure captions

Figure 1 : X-Ray diffractograms obtained at room temperature for $Cr_2Al_xGe_{1-x}C$ compounds. The residual of the refinement, i.e., the difference between the experimental diffractogram and that deduced from Rietveld refinement is given below every diffractogram.

Figure 2 : In $Cr_2Al_xGe_{1-x}C$ compounds, evolution as a function of the Al content (x) of the a and c lattice parameters ((a) and (b) respectively), the relative change of a, c, c/a and the unit cell volume (c), the height of the Cr atom z_{Cr} in the unit cell (d), the distortion factors O_d and P_d (e). the relative change of the distance between Cr atoms and A (Al and/or Ge) atoms or C atoms (f).

Figure 3: Evolution of the a and c lattice parameters, (a) and (b), as a function of the temperature. Deduced linear thermal expansion coefficients along the a and c axis (α_a and α_c) are given in (c).

Figure 4: Evolution of the *a* and *c* lattice parameters of $Cr_5Ge_3C_x$ as a function of temperature

Figure 1

Click here to download high resolution image

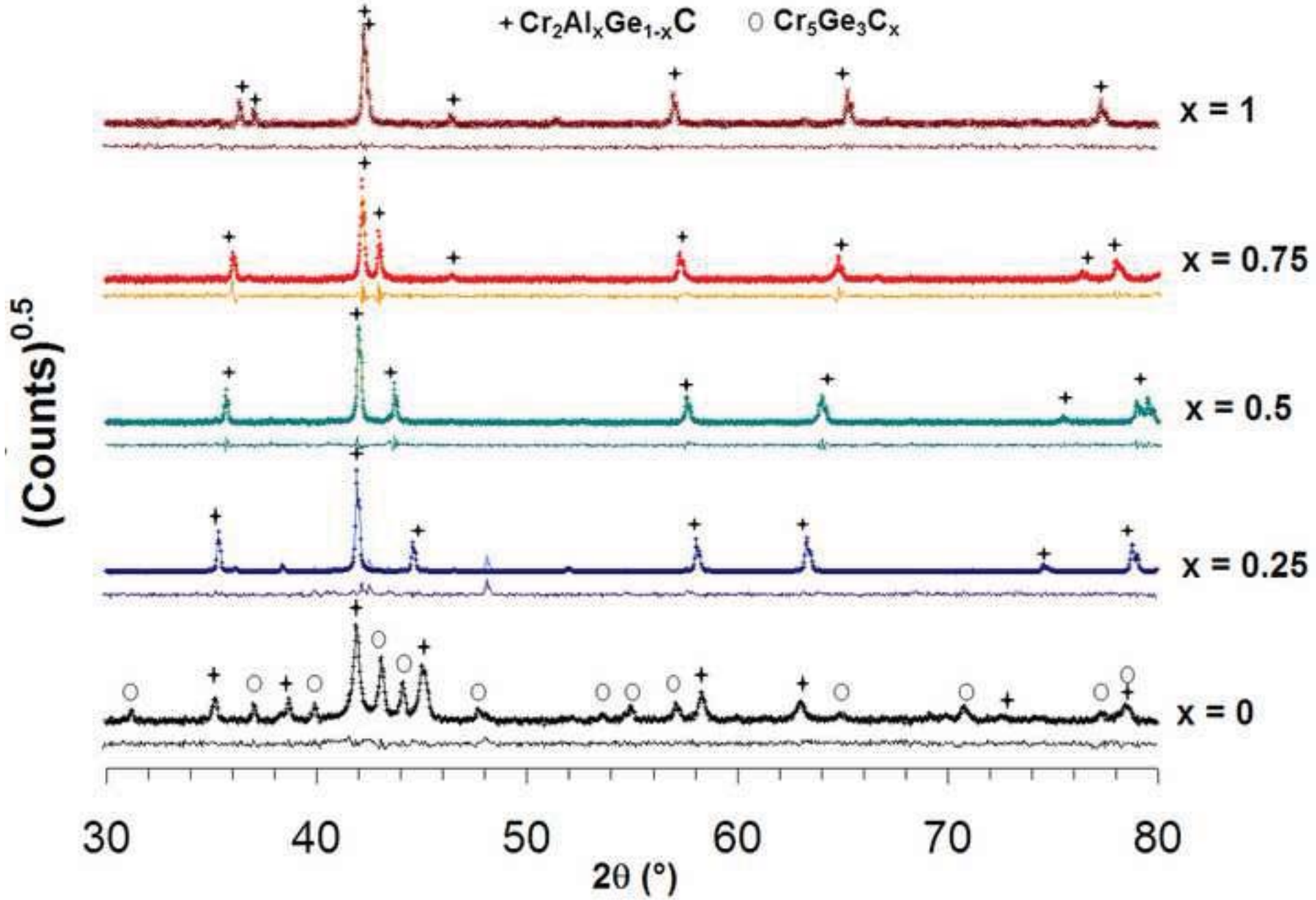

Figure 2a
Click here to download high resolution image

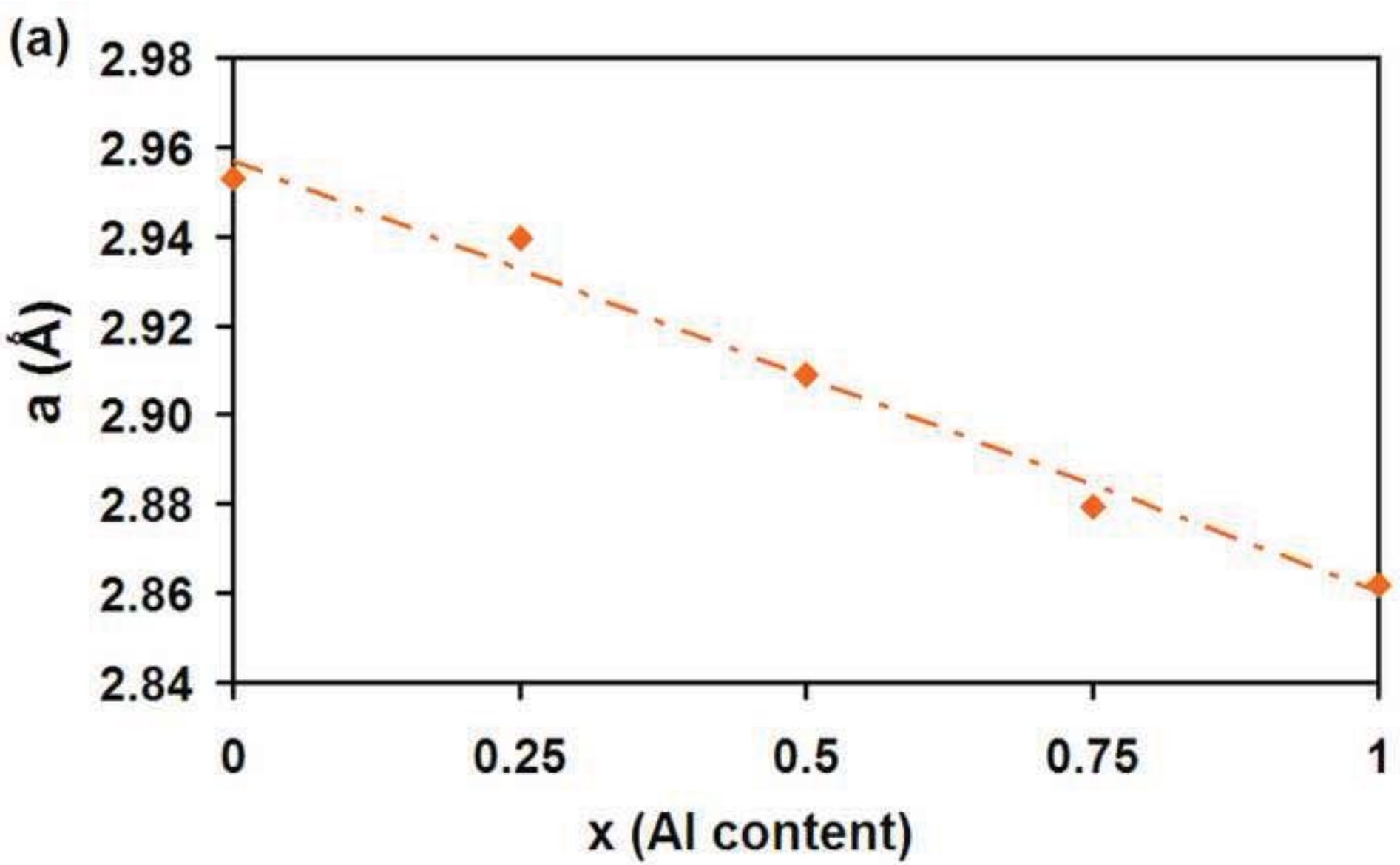

Figure 2b
Click here to download high resolution image

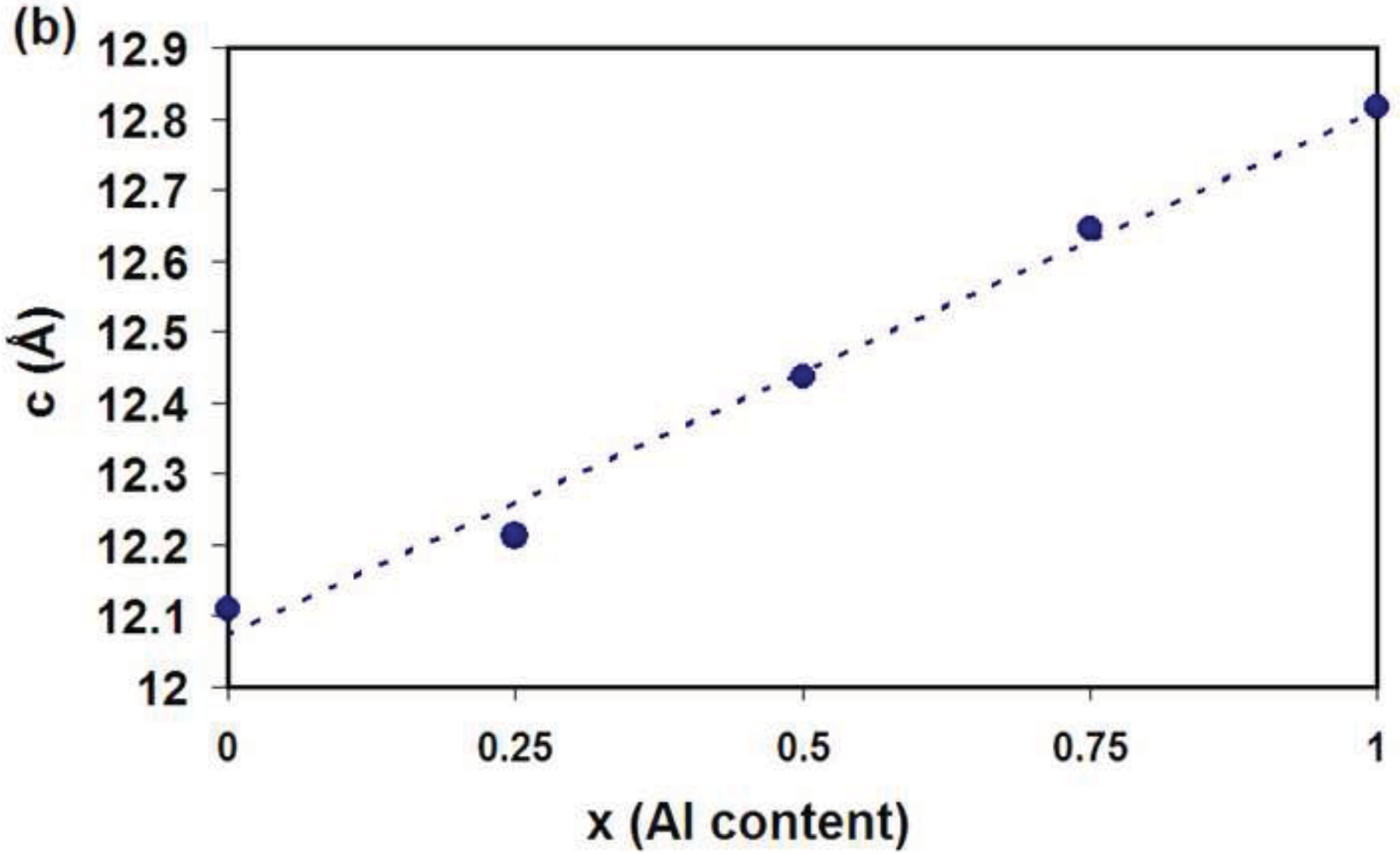

Figure 2c
Click here to download high resolution image

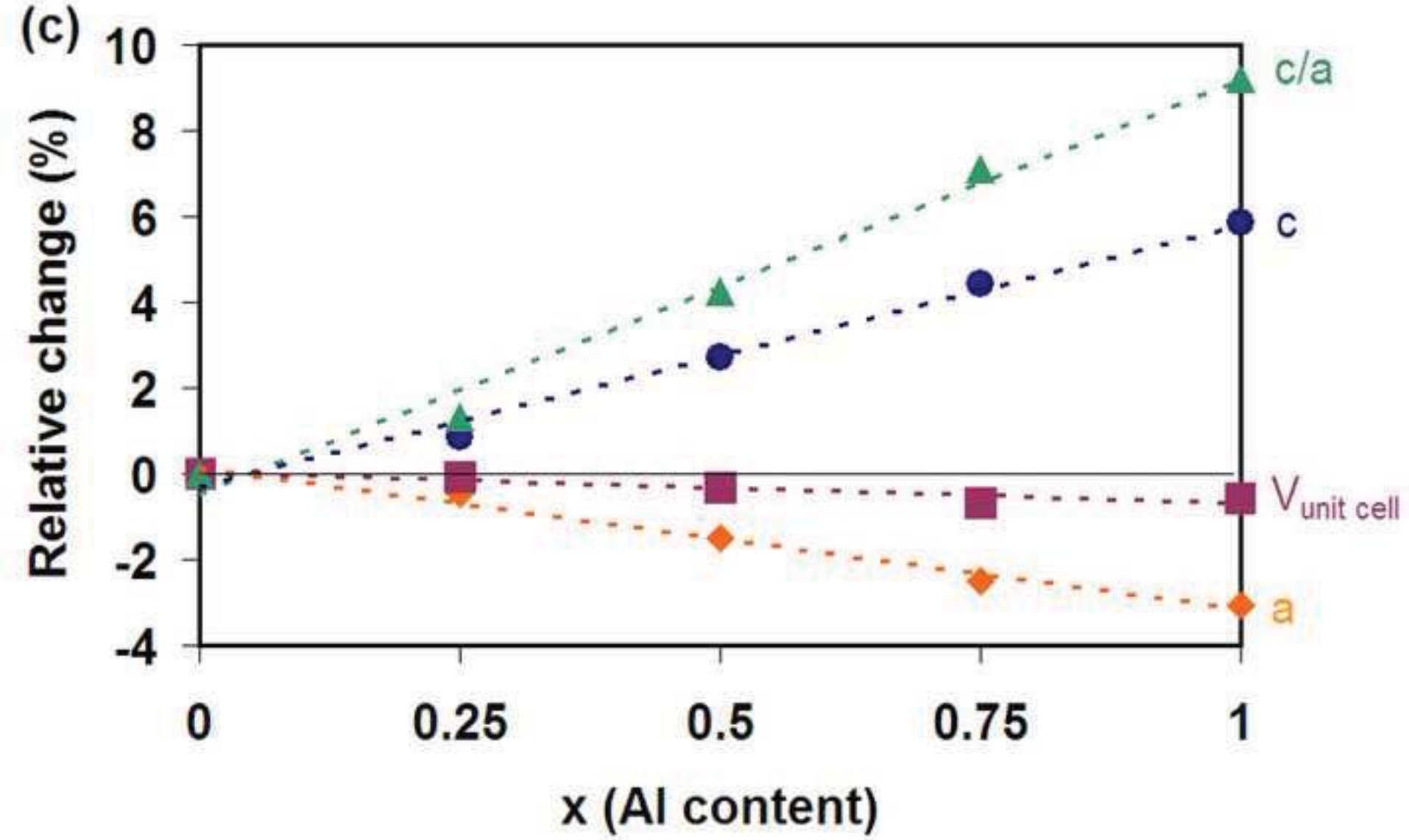

Figure 2d
Click here to download high resolution image

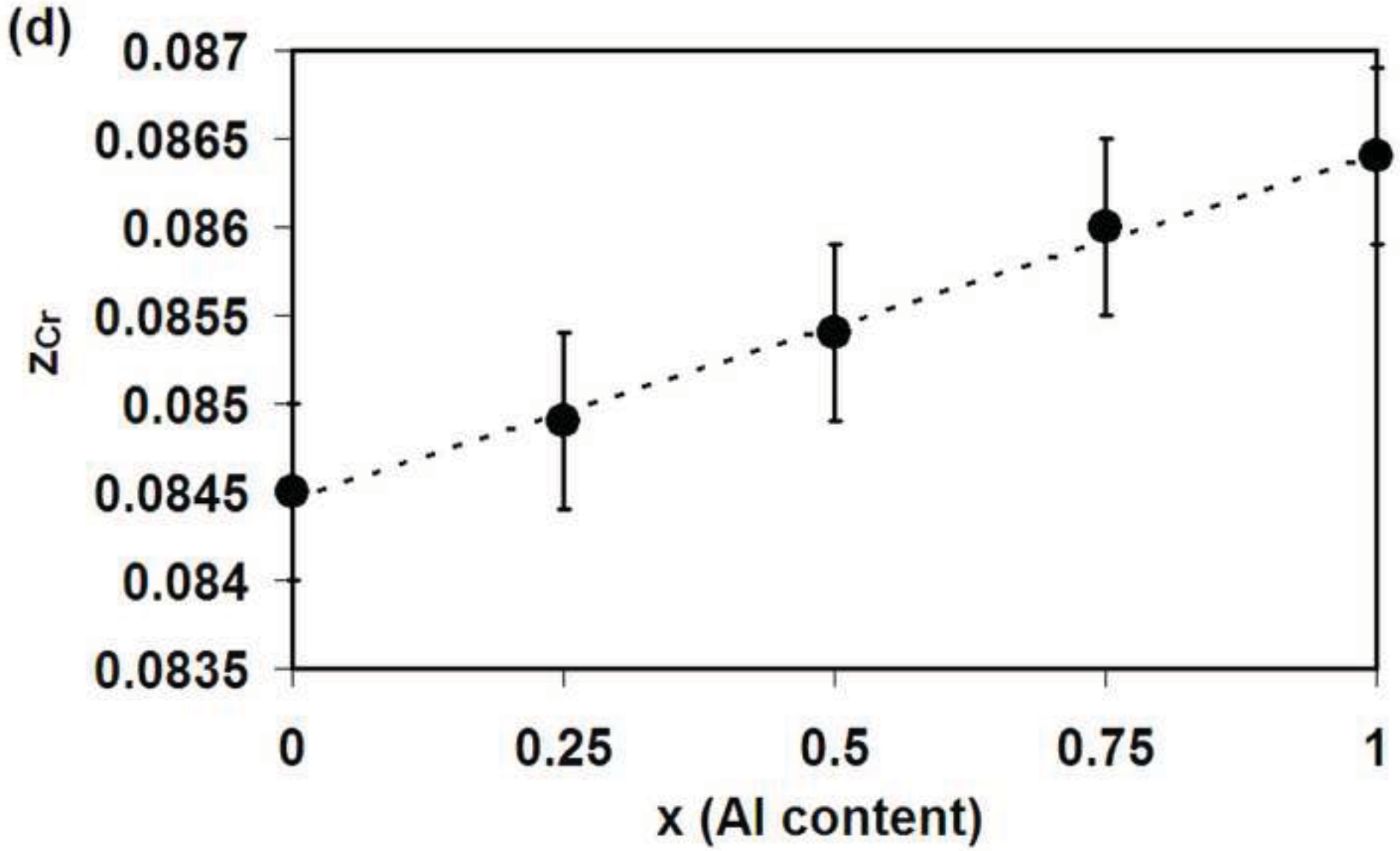

Figure 2e
Click here to download high resolution image

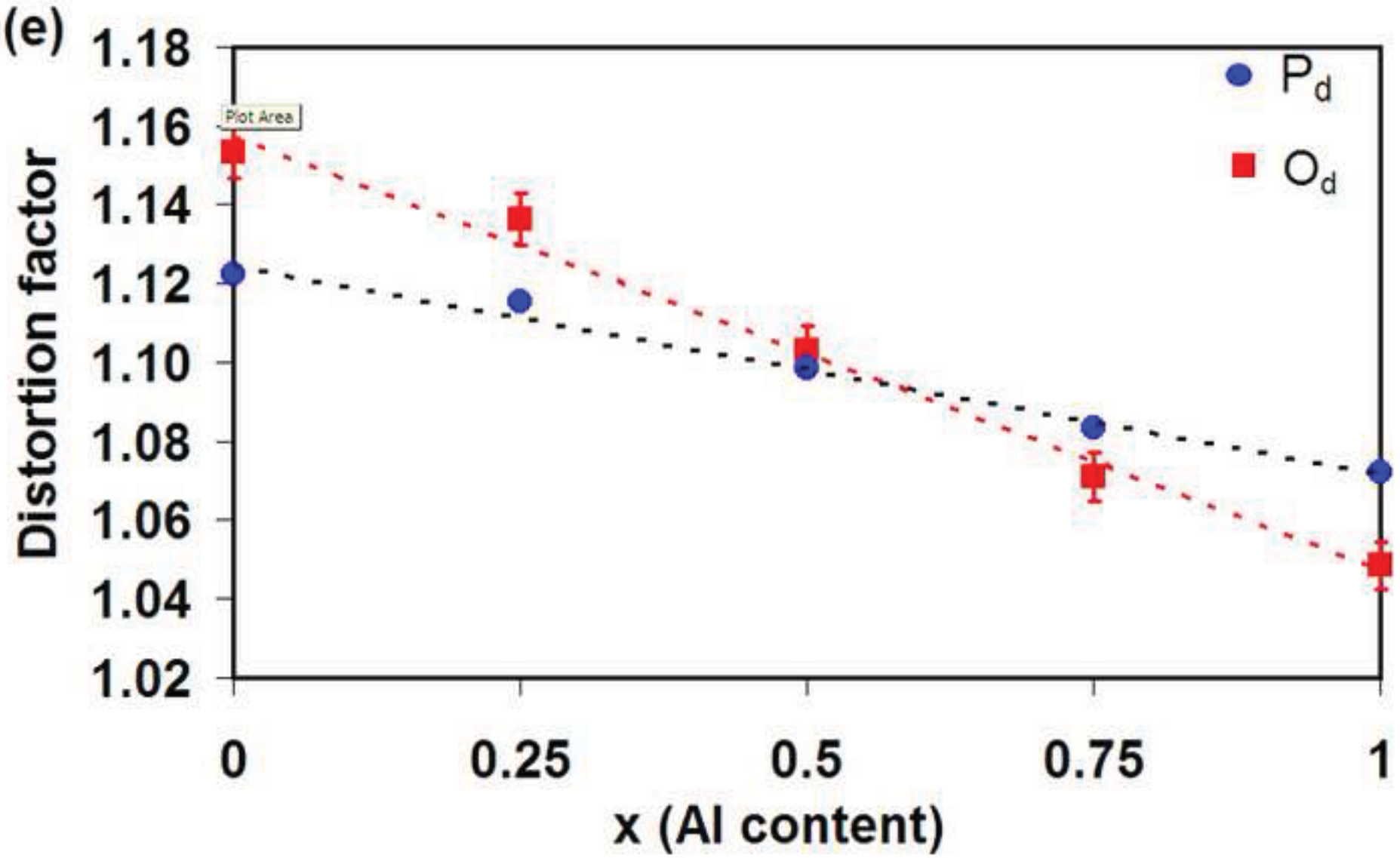

Figure 2f
Click here to download high resolution image

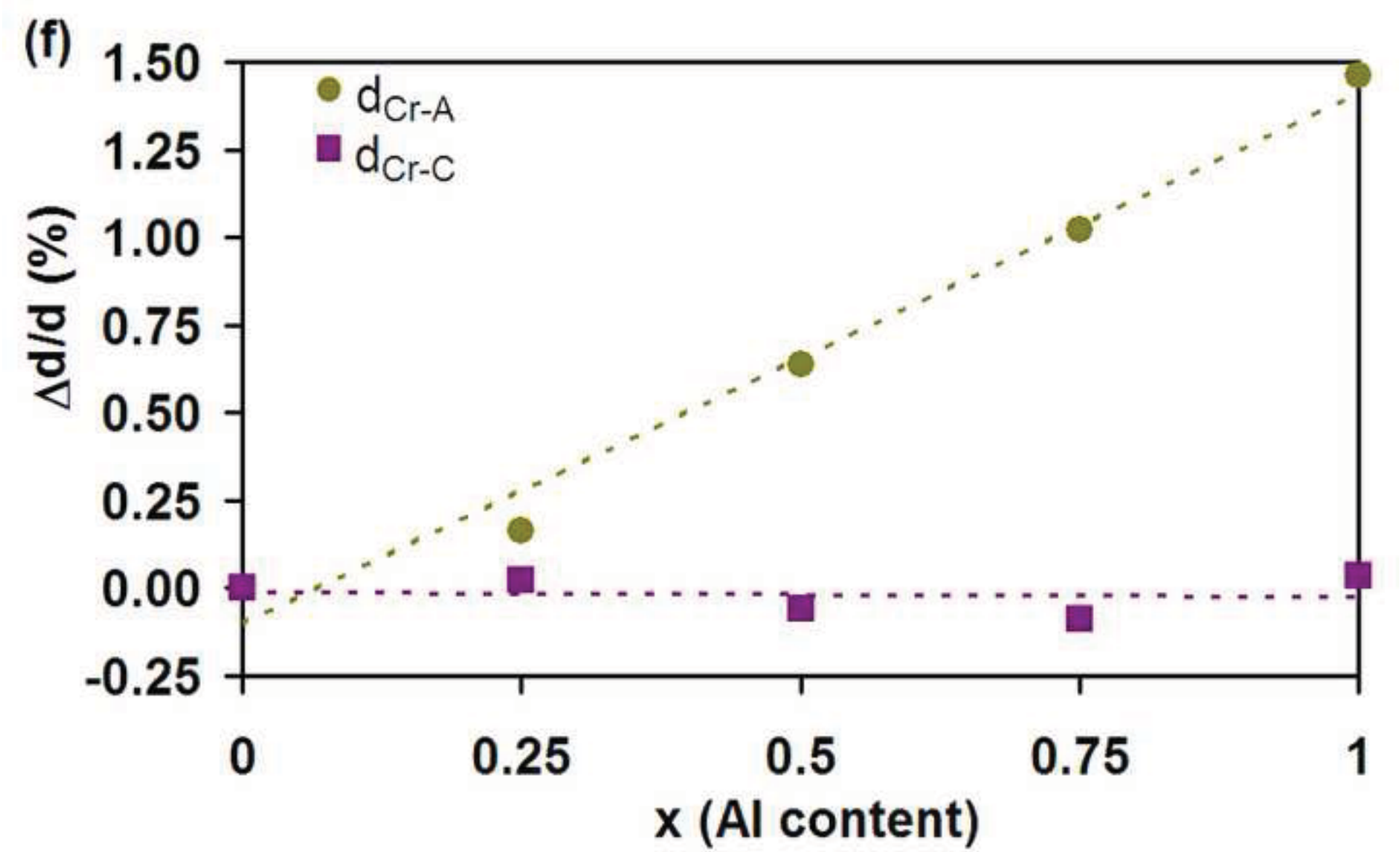

Figure 3a
Click here to download high resolution image

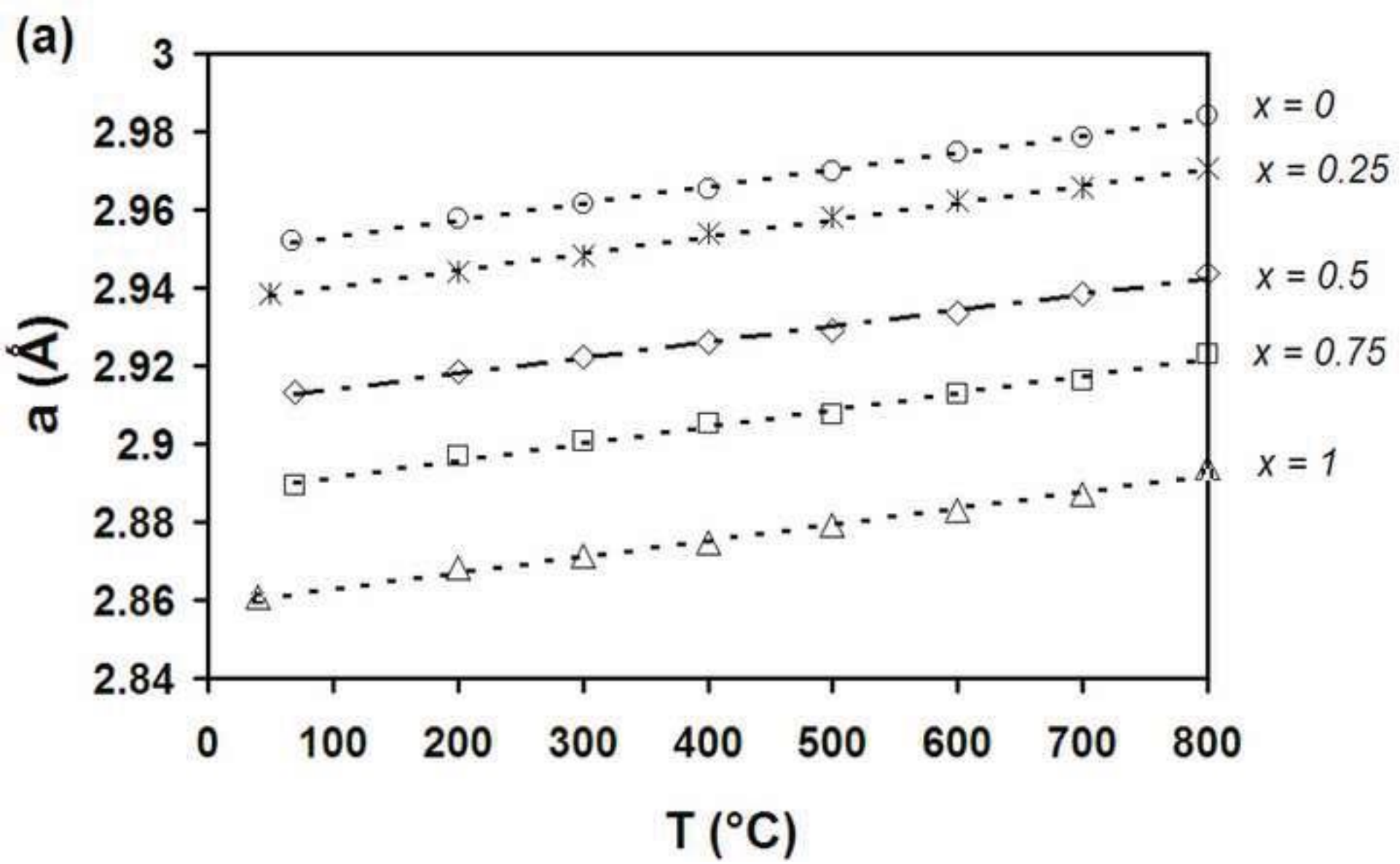

Figure 3b
Click here to download high resolution image

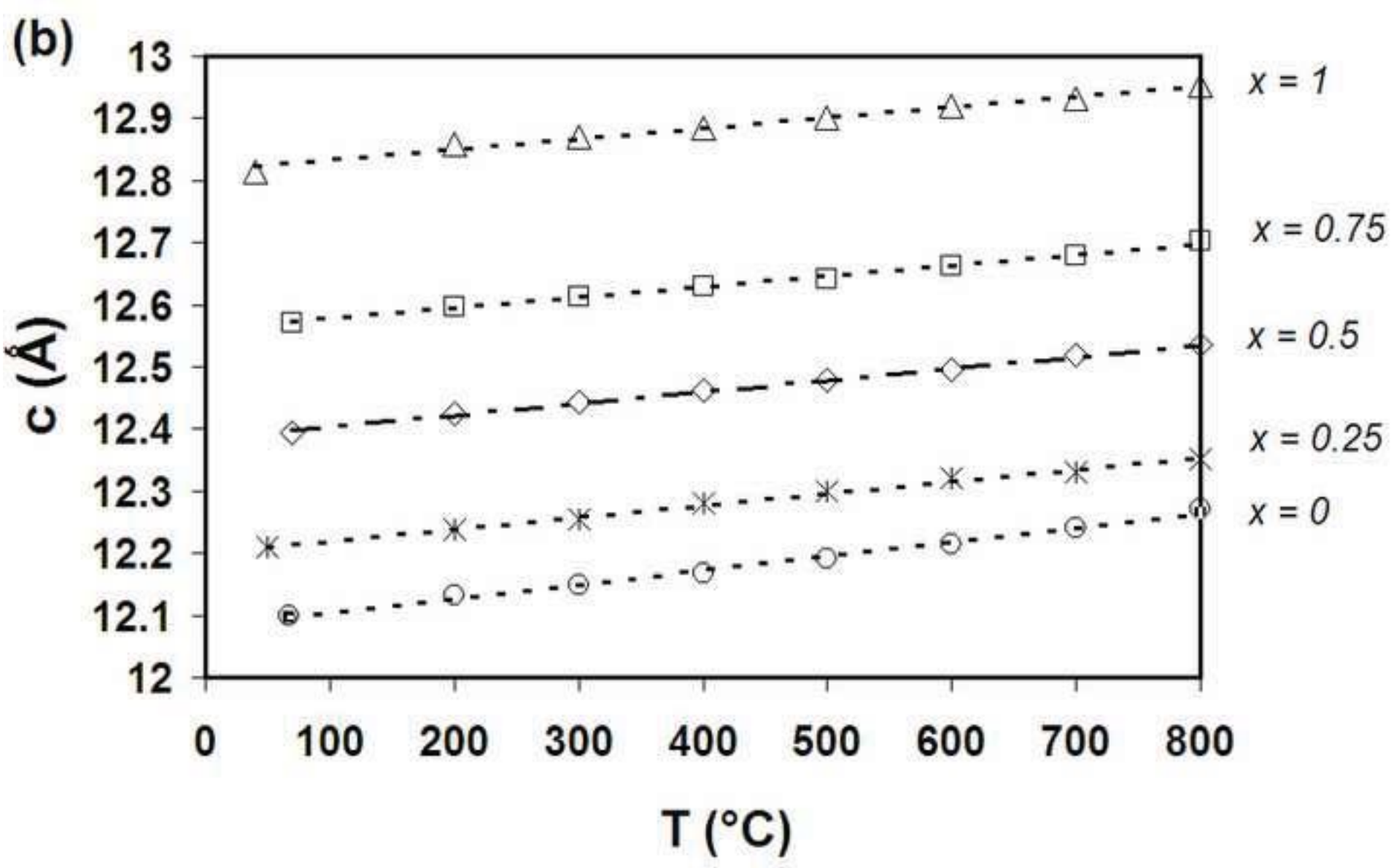

Figure 3c
Click here to download high resolution image

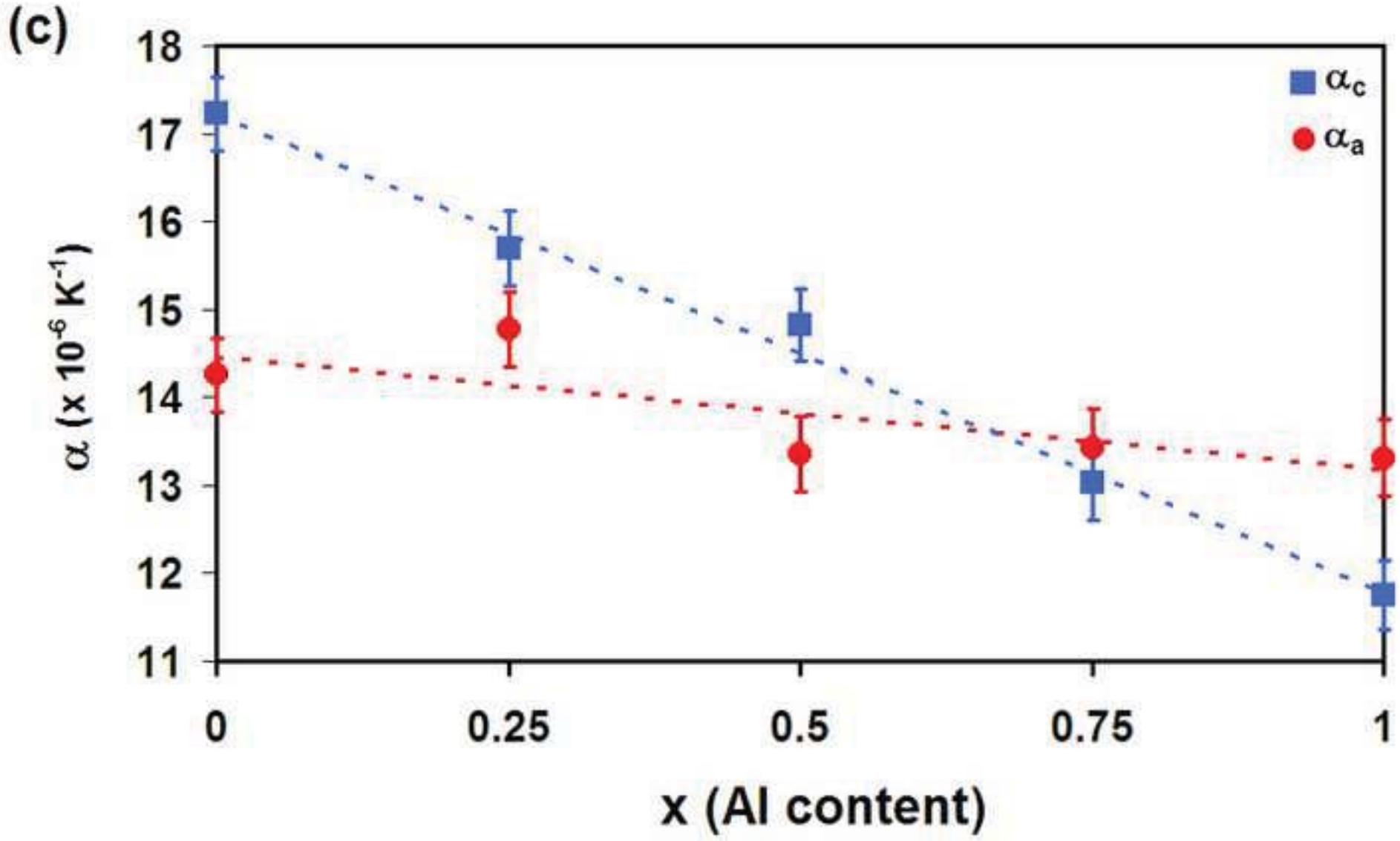

Figure 4

Click here to download high resolution image